

Alternative model of the Antonov problem

L. Velazquez^{1,*} and F. Guzmán^{2,†}

¹*Departamento de Física, Universidad de Pinar del Río,
Martí 270, Esq. 27 de Noviembre, Pinar del Río, Cuba.*

²*Departamento de Física Nuclear, Instituto Superior de Ciencias y Tecnología Nucleares,
Carlos III y Luaces, Plaza, La Habana, Cuba.*

(Dated: May 22, 2019)

Abstract

Astrophysical systems will never be in a real Thermodynamic equilibrium: they undergo an evaporation process due to gravity is not able to confine the particles. Ordinarily this difficulty is overcome by enclosing the system in a rigid container which avoid the evaporation. In the present paper we proposed an energetic prescription which is able to confine the particles, leading in this way to an alternative version of the Antonov isothermal model. In this case, system finite profiles appear, being these characterized by exhibiting an isothermal core with a polytropic halo. Besides of the main features of the isothermal sphere model: the existence of the gravitational collapse and the energetic region with a negative specific heat, this alternative model leads to the existence of upper bound for the total energy where the system is so extremely diluted that the gravity is not able to confine them.

PACS numbers: 05.20.-y; 05.70.-a

I. INTRODUCTION

Thermodynamical properties of selfgravitating systems are very different from the ones exhibited by the traditional systems. They are typical *nonextensive systems* since they are nonhomogeneous and the total energy is not extensive, which is a consequence of the long-range character of gravitational interaction. In recent papers [1, 2] we proved that the selfgravitating systems obey to the following thermodynamic limit:

$$N \rightarrow \infty, \text{ keeping constant } \frac{E}{N^{\frac{7}{3}}} \text{ and } LN^{\frac{1}{3}}, \quad (1)$$

being N , E and L , the number of particles, the total energy and the characteristic linear dimension of the system respectively. As already discussed in ref.[2], the consideration of this thermodynamic limit allows us explain the origin of *dynamical anomalies* in their numerical simulations, such as reduction of mixing and slow relaxation towards the equilibrium [3, 4, 5, 6, 7].

It is well-known that self-gravitating systems exhibit energetic regions with a *negative specific heat*, which persist even in the thermodynamic limit [8, 9, 10, 11, 12, 13, 14, 15]. That is the reason why the Gibbs canonical ensemble is nonapplicable to the description of selfgravitating systems. At first glance, selfgravitating systems could only be described by using the microcanonical ensemble. However, we showed in ref.[1] that geometrical aspects of the probabilistic distribution functions of the ensembles allow us to carry out a well-defined canonical-like description for selfgravitating systems which is equivalent to the microcanonical one. This interesting possibility allows

us to enhance the applicability of a generalized canonical description to a huge world of nonextensive Hamiltonian systems: those exhibiting an exponential growing of the microcanonical accessible volume W with N in the thermodynamic limit [1, 2, 16, 17, 18, 19].

Gravitation is not able to confine the particles: it is always possible that some of them have the sufficient energy for escaping out from the system, so that, the selfgravitating systems always undergo an evaporation process. Therefore, they will never be in a real thermodynamic equilibrium. This difficulty is usually avoided by enclosing the system in a rigid container [12, 13, 14], which could be justified when the evaporation rate is small and certain kind of quasistationary state might be reached.

The use of the rigid container can be conveniently substituted by imposing the following energetic prescription:

$$\frac{1}{2m}p^2 + m\phi(\mathbf{r}) < 0, \quad (2)$$

where $\frac{1}{2m}p^2$ is the kinetic energy of a particle of mass m , being $m\phi(\mathbf{r})$ its gravitational potential energy at the point \mathbf{r} . All those particles satisfying the condition (2) are confined by the gravity, on contrary, they will be able to scape out from the system if they do not lose their excessive energy. When the evaporation rate is small and can be disregarded, the condition (2) acts as a renormalization prescription which leads to finite configurations with an isothermal core with a polytropic halo. Thus, the use of this renormalization procedure is more realistic than the box renormalization (the use of the rigid container). It can be note that this renormalization procedure keeps a closely relation with the energy truncation used in Michie-King model for globular clusters [20]. The aim of this paper is to develop an alternative model to the standard isothermal sphere model of Antonov [12] based on the consideration of this energetic prescription.

*Electronic address: luisberis@geo.upr.edu.cu

†Electronic address: guzman@info.isctn.edu.cu

II. STATISTICAL DESCRIPTION

Let us consider the N -body selfgravitating Hamiltonian system:

$$H_N = T_N + U_N = \sum_{k=1}^N \frac{1}{2m} \mathbf{p}_k^2 - \sum_{j>k=1}^N \frac{Gm^2}{|\mathbf{r}_j - \mathbf{r}_k|}. \quad (3)$$

Taking into consideration the above renormalization prescription (2), the admissible stages of this system are those in which the kinetic energy of a given particle satisfies the condition:

$$\frac{1}{2m} \mathbf{p}_k^2 < u_k = -m\phi(\mathbf{r}_k), \quad (4)$$

being $\phi(\mathbf{r}_k)$ the gravitational potential at the point \mathbf{r}_k where the k -th particle is located:

$$\phi(\mathbf{r}_k) = - \sum_{j \neq k}^N \frac{Gm^2}{|\mathbf{r}_k - \mathbf{r}_j|}. \quad (5)$$

The renormalized microcanonical accessible volume W_R is given by:

$$W_R = \frac{1}{N!} \int_{X_R} \delta[E - H_N] dX,$$

where X_R is a subspace of the N -body phase-space where the condition (4) takes place, being $dX = d^{3N} R d^{3N} P / (2\pi\hbar)^{3N} = \prod_k \frac{d^3 \mathbf{r}_k d^3 \mathbf{p}_k}{(2\pi\hbar)^3}$ the volume element.

This integral is rewritten by using the Fourier representation of the delta function as follows:

$$W_R = \int_{-\infty}^{+\infty} \frac{dk}{2\pi} \exp(zE) \mathcal{Z}_R(z, N), \quad (6)$$

where $\mathcal{Z}_R(z, N)$:

$$\mathcal{Z}_R(z, N) = \frac{1}{N!} \int_{X_R} \exp(-zH_N) dX, \quad (7)$$

is the canonical partition function with complex argument $z = \beta + ik$, with $\beta \in \Re$. Integration by $d^{3N} P$ yields:

$$\frac{1}{N!} \int_{\Re^{3N}} d^{3N} R \left(\frac{m}{2\pi\hbar^2 z} \right)^{\frac{3}{2}N} \exp[-zU_N(R) + \chi(R; z)], \quad (8)$$

being $\chi(R; z)$:

$$\chi(R; z) = \sum_{k=1}^N \ln F[\sqrt{zu_k}]. \quad (9)$$

where $F(z)$ is defined by:

$$F(z) = \operatorname{erf}(z) - \frac{2}{\sqrt{\pi}} z \exp(-z^2). \quad (10)$$

and shown in the Fig.(1). The asymptotic behaviors of $F(z)$ are given by:

$$F(z) = \begin{cases} \frac{4}{3\sqrt{\pi}} z^3 + O(z^3) & \text{when } z \rightarrow 0 \\ \sim 1 & z \geq 2.5 \end{cases}. \quad (11)$$

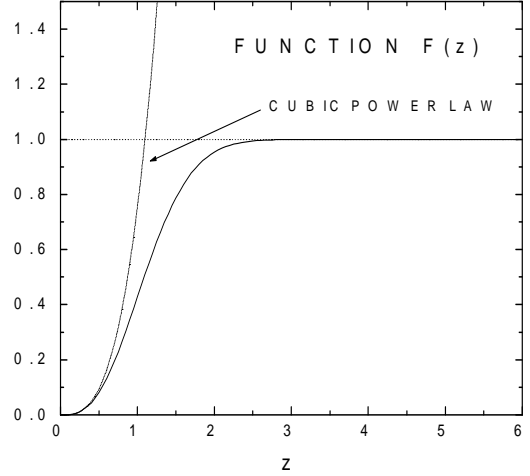


FIG. 1: Representation of the function $F(z)$. Its symptotic behaviors are also shown.

We are interested in describing the large N limit. This aim can be carried out by using following procedure: we partition the physical space in cells $\{c_\alpha\}$ being \mathbf{r}_α the positions of their centers. We denoted by $n_\alpha = n(\mathbf{r}_\alpha)$ the number of particles inside the cell at the position \mathbf{r}_α . Introducing the density $\rho(\mathbf{r}_\alpha) = n(\mathbf{r}_\alpha)/v_\alpha$, being v_α the volume of the cell c_α , the functions $U_N(R)$ and $\chi(R; z)$ are rewritten by using a *mean field approximation* as follows:

$$U_N(R) \longrightarrow U[\rho, \phi] = \int_{\Re^3} \frac{1}{2} m \rho(\mathbf{r}) \phi(\mathbf{r}) d^3 \mathbf{r}, \quad (12)$$

$$\chi(R; z) \longrightarrow \chi[\rho, \phi; z] = \int_{\Re^3} \rho(\mathbf{r}) \ln F\left(\sqrt{-zm\phi(\mathbf{r})}\right) d^3 \mathbf{r}, \quad (13)$$

being $\phi(\mathbf{r})$ the Newtonian potential for a given ρ profile:

$$\phi(\mathbf{r}) = \mathcal{G}[\rho] = - \int_{\Re^3} \frac{Gm\rho(\mathbf{r}_1) d^3 \mathbf{r}_1}{|\mathbf{r} - \mathbf{r}_1|}. \quad (14)$$

which is the Green solution of the problem:

$$\Delta\phi = 4\pi G\rho. \quad (15)$$

Using the partition of the physical space in cells, the integration by $d^{3N}R$ can be approximately given by:

$$\frac{1}{N!} \int_{\mathbb{R}^{3N}} d^{3N}R \simeq \sum_{\{n_\alpha\}} \delta_D \left(N - \sum_\alpha n_\alpha \right) \prod_\alpha \frac{v_\alpha^{n_\alpha}}{n_\alpha!}, \quad (16)$$

where:

$$\delta_D(n) = \begin{cases} 1, & \text{if } n = 0 \\ 0 & \text{otherwise} \end{cases} \quad \text{and} \quad \sum_{\{n_\alpha\}} \equiv \sum_{n_1} \sum_{n_2} \cdots \quad (17)$$

The following factor can be rephrased in the mean field approximation as follows:

$$\left(\frac{m}{2\pi\hbar^2 z} \right)^{\frac{3}{2}N} \prod_\alpha \frac{v_\alpha^{n_\alpha}}{n_\alpha!} \rightarrow e^{-p_f[\rho, z]}, \quad (18)$$

being

$$p_f[\rho, z] = \int_{\mathbb{R}^3} d^3\mathbf{r} \rho(\mathbf{r}) \left[\ln \rho(\mathbf{r}) - 1 + \frac{3}{2} \ln \left(\frac{2\pi\hbar^2 z}{m} \right) \right], \quad (19)$$

where the Stirling formula $\ln n! \simeq n \ln n - n$ was used. Finally, we rephrase the summation in the mean field approximation as follows:

$$\sum_{\{n_\alpha\}} \delta_D \left(N - \sum_\alpha n_\alpha \right) \rightarrow \int \mathcal{D}\rho(\mathbf{r}) \delta \left[N - \int_{\mathbb{R}^3} d^3\mathbf{r} \rho(\mathbf{r}) \right]. \quad (20)$$

Taking into consideration all approximations introduced above, the canonical partition function (7) is rewritten as:

$$\mathcal{Z}_c[z, N] = \int \mathcal{D}\rho(\mathbf{r}) \delta[N - N[\rho]] \times \exp \{ -p_f[\rho, z] - zU[\rho, \phi[\rho]] + \chi[\rho, \phi[\rho]; z] \}, \quad (21)$$

being $N[\rho]$ the number of particles functional:

$$N[\rho] = \int_{\mathbb{R}^3} d^3\mathbf{r} \rho(\mathbf{r}). \quad (22)$$

In order to avoid the complicate ρ dependence of $\phi[\rho]$ in (21), we introduce the identity:

$$\int \mathcal{D}\phi(\mathbf{r}) \delta \{ \phi(\mathbf{r}) - \mathcal{G}[\rho] \} = 1, \quad (23)$$

in the functional integral (21):

$$\int \mathcal{D}\rho(\mathbf{r}) \mathcal{D}\phi(\mathbf{r}) \delta \{ \phi(\mathbf{r}) - \mathcal{G}[\rho] \} \delta(N - N[\rho]) \times \exp \{ -p_f[\rho; z] - zU[\rho, \phi] + \chi[\rho, \phi; z] \}. \quad (24)$$

The delta functions are also convenient rewritten by using their Fourier representation:

$$\delta \{ \phi(\mathbf{r}) - \mathcal{G}[\rho] \} \sim \int \mathcal{D}h(\mathbf{r}) \exp \left[\int_{\mathbb{R}^3} d^3\mathbf{r} J(\mathbf{r}) \{ \phi(\mathbf{r}) - \mathcal{G}[\rho] \} \right], \quad (25)$$

as well as

$$\delta(N - N[\rho]) = \int_{-\infty}^{+\infty} \frac{dq}{2\pi} \exp \{ z_1 (N - N[\rho]) \}, \quad (26)$$

being $z_1 = \mu + iq$ with $\mu \in \mathfrak{R}$; $J(\mathbf{r}) = j(\mathbf{r}) + ih(\mathbf{r})$, a complex function with $j(\mathbf{r})$ and $h(\mathbf{r}) \in \mathfrak{R}$. Thus, the canonical partition function $\mathcal{Z}_c[z, N]$ is finally expressed as:

$$\int_{-\infty}^{+\infty} \frac{dq}{2\pi} \int \mathcal{D}\rho(\mathbf{r}) \mathcal{D}\phi(\mathbf{r}) \mathcal{D}h(\mathbf{r}) \exp \{ z_1 N - H[\rho, \phi; z, z_1, J] \}. \quad (27)$$

The functional $H[\rho, \phi; z, z_1, J]$ is given by:

$$= p_f[\rho; z] + zU[\rho, \phi] - \chi[\rho, \phi; z] + z_1 N[\rho] + K[\phi, \rho, J], \quad (28)$$

being $K[\phi, \rho, J]$ the exponential argument of the expression (25).

According to the thermodynamic limit (1), when N is scaled as $N \rightarrow \alpha N$, the following quantities should be scaled as follows:

$$\rho \rightarrow \alpha^2 \rho, \quad \mathbf{r} \rightarrow \alpha^{-\frac{1}{3}} \mathbf{r}, \quad \phi \rightarrow \alpha^{\frac{4}{3}} \phi, \quad z \rightarrow \alpha^{-\frac{4}{3}} z, \quad (29)$$

where z_1 and $J(\mathbf{r})$ do not change. It can be checked that all terms in (28) scale proportional to α , and therefore:

$$H[\rho, \phi; z, z_1, J] \rightarrow \alpha H[\rho, \phi; z, z_1, J]. \quad (30)$$

The thermodynamic limit is carry out tending α to the infinity, $\alpha \rightarrow \infty$. Thus, we can estimate $\mathcal{Z}_c[z, N]$ for N large by using the *steepest decent method*. The Planck potential $\mathcal{P}(\beta, N) = -\ln \mathcal{Z}_c[\beta, N]$ is obtained as follows:

$$\mathcal{P}[\beta, N] = - \min_{\rho, \phi, \mu, j} [\mu N - H[\rho, \phi; \beta, \mu, j]]. \quad (31)$$

where the stationary conditions:

$$\frac{\delta H}{\delta \rho} = \frac{\delta H}{\delta \phi} = \frac{\delta H}{\delta j} = \frac{\delta H}{\delta \mu} - N = 0, \quad (32)$$

lead to the following relations:

$$\rho = \left(\frac{m}{2\pi\hbar^2\beta} \right)^{\frac{3}{2}} \exp \left[-\mu - \frac{1}{2}\beta m\phi + \mathcal{G}[j] \right] F \left[\sqrt{-\beta m\phi} \right], \quad (33)$$

$$j = -\frac{1}{2}\beta m\rho + \rho \partial_\phi \ln F \left[\sqrt{-\beta m\phi} \right], \quad (34)$$

$$\phi = \mathcal{G}[\rho] \text{ and } N = N[\rho], \quad (35)$$

The relations (33) and (34) define the state equation; the relations (35) establish the Newtonian potential ϕ for a given ρ profile, being this identical to (14), as well as the normalization constrain for the number of particles. The relation (33) is conveniently rewritten by using (34) as follows:

$$\rho = N(\beta, \mu) \exp[\Phi + C] F \left(\Phi^{\frac{1}{2}} \right), \quad (36)$$

where $\Phi = -\beta m\phi$ and $N(\beta, \mu) = \left(\frac{m}{2\pi\hbar^2\beta} \right)^{\frac{3}{2}} \exp(-\mu)$, being C a new function which is given by:

$$C = -\beta m\mathcal{G} \left[\rho \partial_\phi \ln F \left(\Phi^{\frac{1}{2}} \right) \right]. \quad (37)$$

It is not difficult to show that the Planck potential is given by:

$$\mathcal{P}(\beta, N) = -1 - \mu + \int_{\mathbb{R}^3} d^3\mathbf{r} \rho \left(\frac{1}{2}\Phi + C \right). \quad (38)$$

The Boltzmann entropy can be estimated by using the steepest decent method as follows:

$$S_B(E, N) = \min_\beta [\beta E - \mathcal{P}[\beta, N]], \quad (39)$$

where the stationary solution satisfies the relation:

$$E = \frac{\partial \mathcal{P}[\beta, N]}{\partial \beta} = E[\beta, \rho, \phi], \quad (40)$$

being $E[\beta, \rho, \phi]$ the energy functional:

$$E[\beta, \rho, \phi] = \int_{\mathbb{R}^3} d^3\mathbf{r} \left[3 - \Phi \partial_\Phi \ln F \left(\Phi^{\frac{1}{2}} \right) \right] \frac{1}{2\beta} \rho + \frac{1}{2} m\rho\phi. \quad (41)$$

It can be easily seen that the quantity:

$$\epsilon(\beta, \Phi) = \left[3 - \Phi \partial_\Phi \ln F \left(\Phi^{\frac{1}{2}} \right) \right] \frac{1}{2\beta}, \quad (42)$$

represents the *kinetic energy per particle* at a given point of the selfgravitating system. Note that ρ vanishes when Φ tends to zero in (36), so that, the particle distribution has been *renormalized*. This state equation differs from the one obtained in the isothermal model by the presence of the truncation function $F \left(\Phi^{\frac{1}{2}} \right)$ as well as the *driving function* C . Although C naturally appears in our derivation, its existence is closely related with the modification provoked in the microscopic picture of the system by the evaporation. An example of this affirmation is the alteration of the Maxwell distribution along the system, which can be noted in the kinetic energy per particle $\epsilon(\beta, \Phi)$ (42). A naive energy truncation of the *Maxwell-Boltzmann distribution*:

$$\omega_{MB} = C_0 \exp \left[-\beta \left(\frac{1}{2m} p^2 + m\phi \right) \right]. \quad (43)$$

leads to the state function:

$$\rho \sim \exp[\Phi] F \left(\Phi^{\frac{1}{2}} \right), \quad (44)$$

but here the driving function C does not appear.

The reader may object that the validity of (40) can not be ensured due to the existence of an energetic region where the system exhibits a negative specific heat. However, we recall that the stationary solutions of microcanonical and the canonical ensemble coincide. Moreover, geometrical aspects of the statistical ensembles also protect these stationary solutions under the *reparametrization changes*, where it is always possible to choose a representation where ensemble equivalence will takes places (see ref.[1]).

III. NUMERICAL STUDY

It is convenient to work with dimensionless quantities in order to perform numerical study of the equations obtained in the previous section. Let us introduce firstly the characteristics units for the present model:

$$\epsilon_0 = 2\pi \frac{G^2 m^5}{\hbar^2}, \quad \rho_0 = (2\pi)^3 \frac{G^3 m^9}{\hbar^6}, \quad L_0 = \frac{1}{2\pi} \frac{\hbar^2}{Gm^3}, \quad (45)$$

as well as to set N as the unity. It is also convenient to work with the dimensionless function Φ instead of the Newtonian potential ϕ , as well as we use ξ coordinate defined by:

$$\xi = \sqrt{\mathcal{K}(\beta, \mu)} r, \quad (46)$$

being $\mathcal{K}(\beta, \mu) = \beta^{-\frac{1}{2}} \exp(-\mu)$.

It is not difficult to show that the functions Φ and C obey to the following structure equations:

$$\Delta_\xi \Phi = -4\pi F_1(C, \Phi), \quad \Delta_\xi C = -4\pi F_2(C, \Phi), \quad (47)$$

where $\Delta_\xi u = \xi^{-2} \partial_\xi (\xi^2 \partial_\xi u)$ is the radial part of the Laplace operator, being:

$$\begin{aligned} F_1(C, \Phi) &= \exp(C + \Phi) F\left(\Phi^{\frac{1}{2}}\right), \\ F_2(C, \Phi) &= \frac{2}{\sqrt{\pi}} \exp(C) \Phi^{\frac{1}{2}}. \end{aligned} \quad (48)$$

The solutions of the nonlinear system (47) satisfy the following condition in the infinity:

$$\lim_{\xi \rightarrow \infty} \Phi(\xi) = \lim_{\xi \rightarrow \infty} C(\xi) = 0, \quad (49)$$

which is derived from the asymptotic behavior of Green solutions (14). The solution of (47) is obtained starting from the imposition of the following boundary conditions at the origin $\xi = 0$:

$$\Phi(0) = \Phi_0 > 0, \quad (50)$$

$$C(0) = C(\Phi_0), \quad (51)$$

where the value of $C(0)$ depends on the parameter Φ_0 because of C must vanish when $\xi \rightarrow \infty$. This situation can be overcome redefining the problem as follows: firstly, displacing the function $C(\xi)$ as follows

$$C(\xi) = -c(\infty) + c(\zeta), \quad \Phi(\xi) = \varphi(\zeta) \quad (52)$$

being $\{\varphi(\zeta), c(\zeta)\}$ the solution of (47) with coordinate ζ whose boundary conditions are given by:

$$\phi(0) = \Phi_0, \quad (53)$$

$$c(0) = 0, \quad (54)$$

where ξ is related with ζ throughout the relation:

$$\xi = \exp\left[\frac{1}{2}c(\infty)\right] \zeta. \quad (55)$$

The normalization constrain for the number of particles in (35) is equivalent to the relation:

$$\beta \sqrt{\mathcal{K}(\beta, \mu)} = -\lim_{\xi \rightarrow \infty} \xi^2 \partial_\xi \Phi(\xi) = h(\Phi_0), \quad (56)$$

which allows us to express μ as a function on β and Φ_0 . Taking into consideration the equations (41), (56)

and (38), the total energy and the Planck potential are rewritten:

$$E(\beta, \Phi_0) = \frac{1}{\beta} \left[\frac{3}{2} - \frac{h_1(\Phi_0)}{h(\Phi_0)} \right], \quad (57)$$

$$\mathcal{P}(\beta, \Phi_0) = -1 - \frac{3}{2} \ln \beta + 2 \ln h(\Phi_0) + \frac{h_2(\Phi_0)}{h(\Phi_0)}, \quad (58)$$

being:

$$h_1(\Phi_0) = \int_0^{+\infty} 4\pi \xi^2 d\xi \Phi \left[F_2(C, \Phi) + \frac{1}{2} F_1(C, \Phi) \right], \quad (59)$$

$$h_2(\Phi_0) = \int_0^{+\infty} 4\pi \xi^2 d\xi F_1(C, \Phi) \left[C + \frac{1}{2} \Phi \right]. \quad (60)$$

We use the relation (40) in order to obtain the Φ_0 dependence of $\beta(\Phi_0)$, from the which is derived the equation:

$$\frac{d \ln \beta(\Phi_0)}{d \Phi_0} = \frac{\partial H(\Phi_0)}{\partial \Phi_0} \left[3 - \frac{h_1(\Phi_0)}{h(\Phi_0)} \right]^{-1}, \quad (61)$$

where:

$$H(\Phi_0) = 2 \ln h(\Phi_0) + \frac{h_2(\Phi_0)}{h(\Phi_0)}. \quad (62)$$

The integration of (61) allows us to obtain $\beta(\Phi_0)$ up to the precision of a non relevant constant factor which we set as the unity. Finally, the entropy of the system (39) is rewritten as follows:

$$S_B[\Phi_0] = \frac{5}{2} + \frac{3}{2} \ln \beta(\Phi_0) - H(\Phi_0) - \frac{h_1(\Phi_0)}{h(\Phi_0)}. \quad (63)$$

IV. RESULTS AND DISCUSSIONS

It is interesting to study the asymptotic characteristics of the state function for the particles density ρ . According to the asymptotic behaviors (11) of the function $F(z)$, the state equation (36) becomes in the *isothermal distribution* when $\Phi > 2.5$:

$$\rho \propto \exp[\Phi], \quad (64)$$

which is characteristic of the inner regions of the system (the core). At local level, the particles velocities obey to the Maxwell distribution with $\beta = \beta(\Phi_0)$, where the kinetic energy per particle (42) is given by $3/2\beta$. When we move from the inner regions towards the outer ones,

the kinetic energy per particle decreases until zero, being this approximately given by $\epsilon \simeq 3\Phi/5\beta$, where the particles velocities obey to an *uniform distribution*. Thus, the state equation in the halo obey to a *polytropic distribution*:

$$\rho \propto \frac{4}{3\sqrt{\pi}}\Phi^{\frac{3}{2}}. \quad (65)$$

All these behaviors appear as consequence of the high energy cutoff (4) in the Maxwell distribution for the kinetic energy $f(k) = 2\pi^{-\frac{1}{2}}k^{\frac{1}{2}}\exp(-k)$ ($k = \beta\mathbf{p}^2/2m$), which is shown in the Fig.(2). Note that the cutoff value of k is equal to Φ . In the inner regions where $\Phi > 2.5$, this energy cutoff is unimportant because of it is located in the tail of the distribution. However, it modifies considerably the character of the state function for ρ in the halo due to it is located before the pick.

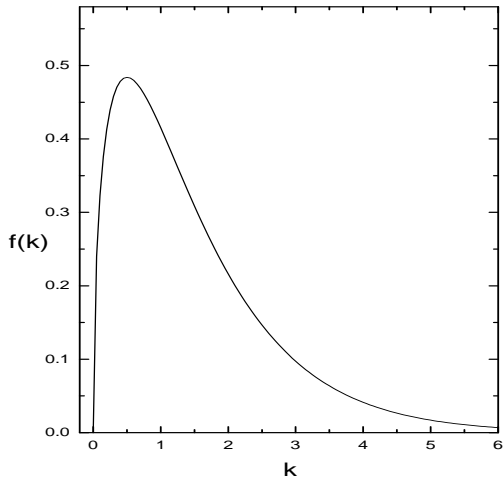


FIG. 2: Maxwell distribution for the kinetic energy. The character of the state function for the particles density ρ depends on the localization of the energy cutoff Φ .

The particle density ρ will obey to the polytropic dependence (65) in all system regions when Φ_0 is small. In this case, the structure equations (47) become in a quasi-polytropic model:

$$\Delta\Phi = -4\pi \exp(C) \frac{4}{3\sqrt{\pi}}\Phi^{\frac{3}{2}}, \quad \Delta C = -4\pi \exp(C) \frac{2}{\sqrt{\pi}}\Phi^{\frac{1}{2}}, \quad (66)$$

which exhibits the same fractal characteristics of a polytropic model with polytropic index $\gamma = \frac{5}{3}$. This polytropic index characterizes an adiabatic process of the ideal gas of particles, which in our case is the evaporation of the system in the vacuum. However, this equation system is not equivalent to polytropic model due to the presence of the driving function C . In order to clarify the effect of the function C , we compare the function $\Phi(\xi)$ obtained from the model (66) with the one obtained without considering the factor $\exp(C)$. This result is showed

in the Fig.(3). Note that the consideration of this term reduces the system size in comparison with the polytropic equation. A non polytropic dependence with $\Phi_0 = 5$ is also shown in order to compare the differences of these three profiles. Note that the system size almost does not depends on Φ_0 in the alternative model.

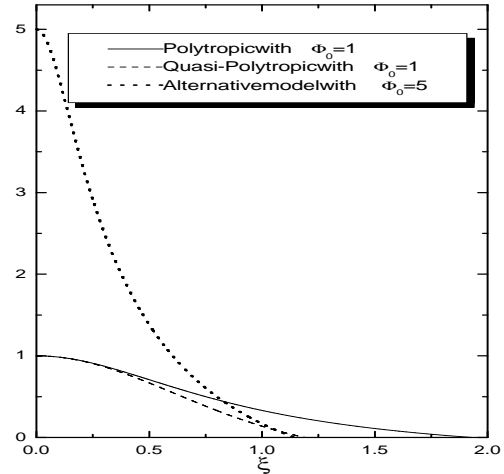


FIG. 3: Influence of the driving function C on $\Phi(\xi)$: Its consideration reduces the system size in comparison with the one obtained in the polytropic model. A nonpolytropic profile with $\Phi_0 = 5$ is also shown.

Let us discuss now the results of the numerical calculations. The Φ_0 -dependence of the functions $h(\Phi_0)$, $h_1(\Phi_0)$ and $h_2(\Phi_0)$ is shown in the Fig.(4). Observe the oscillatory character of these functions with the increasing of the parameter Φ_0 .

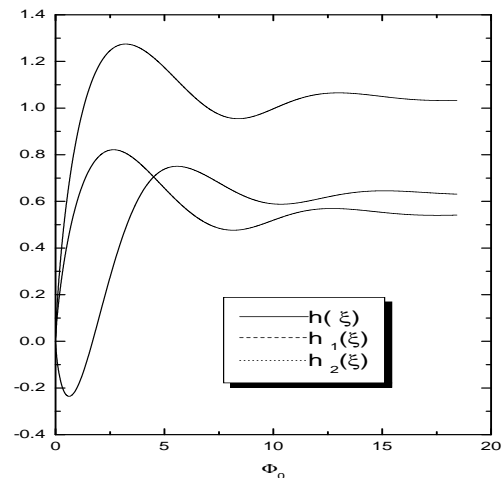


FIG. 4: The functions $h(\Phi_0)$, $h_1(\Phi_0)$ and $h_2(\Phi_0)$.

We obtained the Φ_0 -dependence of the canonical parameter $\beta(\Phi_0)$ and the total energy $E(\Phi_0)$ throughout the equation (61). We also studied the radio in which is contained the 80 % of the total mass of the system,

$R_{80\%}$, as well as for the central density ρ_0 as functions of Φ_0 . All these dependencies are shown in the figures (5), (6), (7) and (8) respectively.

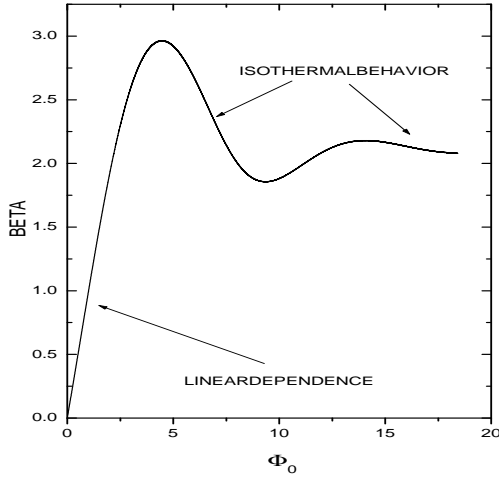


FIG. 5: Canonical parameter β versus Φ_0 . The linear dependence is characteristic of the quasi-polytropic distribution while the oscillatory one is characteristic of the isothermal distribution.

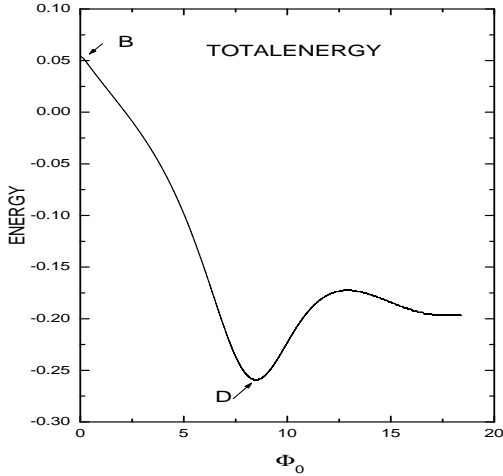


FIG. 6: Total energy E versus Φ_0 . It shows that the total energy for equilibrium configurations is delimited.

Let us to comment briefly these results. At the first glance, it is notable the delimited character of the functions $\beta(\Phi_0)$, $E(\Phi_0)$ and $R_{80\%}(\Phi_0)$ for all the values of the variable Φ_0 : all of them are enclosed in the following intervals:

$$\beta \in (0, 2.99); E \in (-0.257, 0.055); R_{80\%} \in (1.02, 1.33), \quad (67)$$

showing an oscillatory behavior for high values of Φ_0 around the values $\beta_\infty \simeq 2.12$, $\epsilon_\infty \simeq -0.18$, and

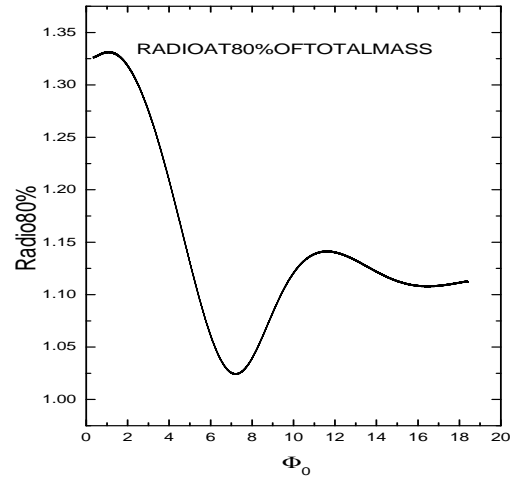


FIG. 7: Radio at the 80% of the system total mass versus Φ_0 . The values of this observable keeps in a narrow interval for all values of Φ_0 .

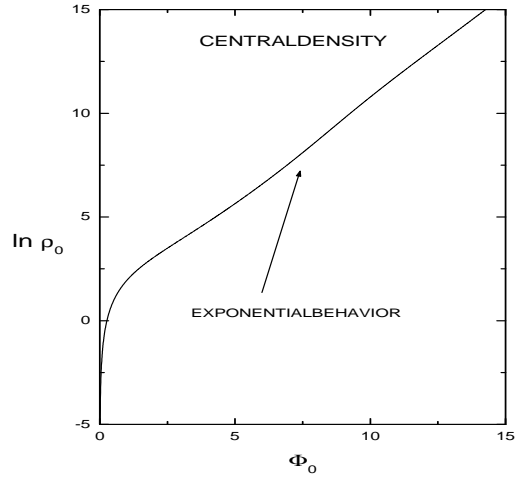


FIG. 8: Central density ρ_0 vs Φ_0 . This function grows monotonically with the increasing of Φ_0 . This result allows us to understand that with the increasing of Φ_0 the system develop a core-halo structure (a high dense core and a dilute halo).

$(R_{80\%})_\infty \simeq 1.11$. However, the central density grows monotonic with the increasing of Φ_0 , exhibiting an exponential behavior for $\Phi_0 > 9.45$. It is very easy to understand that our solution also exhibits the features of the isothermal model of Antonov [12]. This is evident when analyzing the dependency β vs E in the Fig.(9): the caloric curve. We found again the very well-known spiral. The Fig.(10) shows the dependence of the radio in which is contained the 80% of the total mass of the system versus its total energy.

All these configurations contained between the points **B** and **C** can be described using the canonical description. Here the system exhibits a positive heat capacity. All the equilibrium configurations between the points **C**

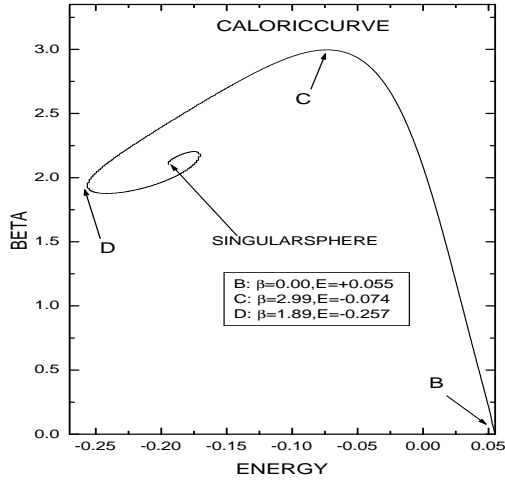


FIG. 9: Caloric curve of the astrophysical system. It is obtained again the classical spiral. In general, the results of the present model exhibit the same features of the Antonov's problem.

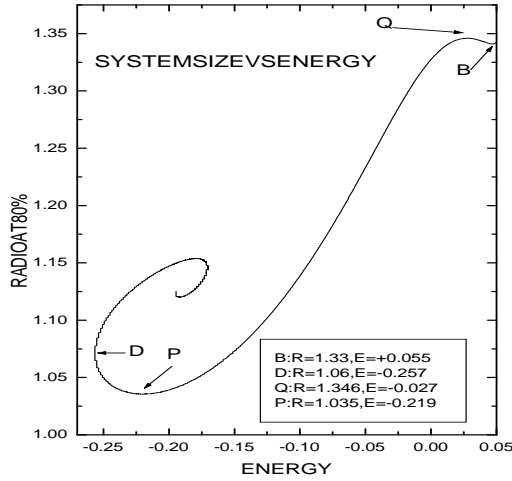


FIG. 10: Ratio at 80% of the total mass versus total energy.

and **D** can not be accessed from the canonical description. In this part of the spiral the systems exhibits a *negative heat capacity*. No equilibrium configurations exists for values of β greater than $\beta_C = 2.99$. Ordinarily this is referred as the *isothermal catastrophe*. On the other hand, no equilibrium configurations exists for energies outside the interval $(-0.26, 0.055)$. For energies greater than $E_B = 0.055$ the system is extreme diluted and can not be confined. For energies below of $E_D = -0.257$, the systems collapse developing a core-halo structure. It is obtained again the *gravothermal catastrophe*. It is interesting to note in the Fig.(10) that the radio in which is enclosed the 80% of the total mass exhibits a weak dependence on the total energy.

All those configurations contained between the points **B** to **D** correspond to equilibrium situations, the other

points of the spiral correspond to unstable saddle points. This is evident when analyzing the thermodynamic potentials of the ensembles. The dependence of the Planck's potential from the canonical parameter β is represented in the Fig.(11). Here it is evident that in the canonical ensemble all those configurations between the points **B** to **C** are stable: *in such points it is minimized this thermodynamic potential for a given β* . In the Fig.(12) we showed that in the microcanonical ensemble all those configurations between the points **B** to **D** are stable: *in such points it is maximized the entropy for each accessible value of the energy*.

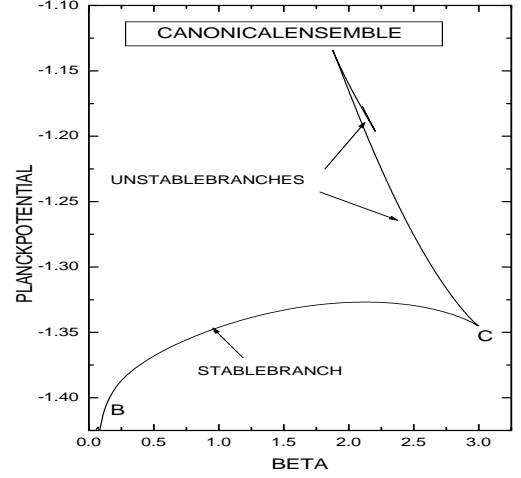


FIG. 11: Canonical ensemble: Planck's Thermodynamical potential versus canonical parameter β . The minimal value for a given β correspond to stable state (all the points of the **B-C** interval).

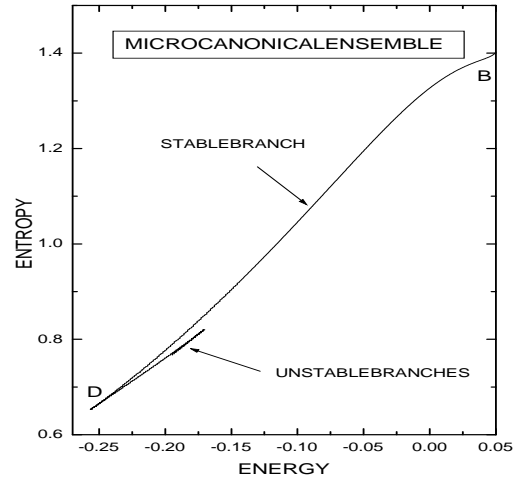


FIG. 12: Microcanonical ensemble: Entropy versus canonical parameter β . The maximal value for a given E corresponds to a stable state (all the points of the **B-D** interval).

The Gibbs' argument, the equilibrium of a subsystem with a thermal bath, is non applicable to this situation

because of no reasonable thermal bath exists for the astrophysical systems. Therefore, the isothermal catastrophe is not a phenomenon with physical relevance since it can never be obtained in the nature: the consideration of a thermal bath in the astrophysical system is outside of context. A different significance possesses the gravothermal catastrophe. The gravitational collapse is the main engine of structuration in astrophysics and it concerns almost all scales of the universe: the formation of planetesimals in the solar nebula, the formation of stars, the fractal nature of the interstellar medium, the evolution of globular clusters and galaxies and the formation of galactic clusters in cosmology [21].

V. CONCLUSIONS

As already shown, the consideration of the energetic prescription (2) leads to an alternative model of the

Antonov problem. This model, besides of exhibiting the all the features of the isothermal model: the gravitational collapse and the energetic region with a negative specific heat, has the advantage that the system size naturally appears. There is no need of enclosing the system in a rigid container in order to avoid the evaporation, since this renormalization procedure is sufficient to confine the system. This approach allows us the consideration of both profiles: the isothermal profile and the polytropic one. The profiles with an isothermal core exhibits always a polytropic halo. With the increasing of the energy, the all system regions will exhibit a polytropic structure, but there is a upper bound for the total energy which imposes a limit for the existence of equilibrium configurations: the system is extremely diluted here, and therefore the gravity is not be able to confine the particles beyond this limit.

-
- [1] L. Velazquez and F. Guzman, e-print (2003) [cond-mat/0303444].
 - [2] L. Velazquez and F. Guzman, e-print (2003) [cond-mat/0303496].
 - [3] M. Cerruti-Sola and M. Pettini, Phys. Rev. E **51**, 53 (1995).
 - [4] A. Taruya and M. Sakagami, e-print (2003) [astro-ph/0303415], accepted paper for publication in Phys. Rev. Lett.
 - [5] A. Campa, A. Giansanti, D. Moroni and C. Tsallis, Phys. Rev. Lett. A **286** (2001) 251.
 - [6] A. Campa, A. Giansanti and D. Moroni, Physica A **305** (2002) 137.
 - [7] I.V. Sideris and H.E. Kandrup, Phys.Rev. E **65** (2002) 066203; e-print (2001) [astro-ph/0111488].
 - [8] T. Padmanabhan, Phys. Rep. **188** , 285 (1990).
 - [9] M. Kiessling, J. Stat. Phys. **55** , 203 (1989).
 - [10] D. Ruelle, Helv. phys. Acta **36** , 183 (1963). M.E. Fisher, Archive for Rational Mechanics and Analysis **17** , 377 (1964).
 - [11] J. van der Linden, Physica **32** , 642 (1966); *ibid* **38** , 173 (1968); J. van der Linden and P. Mazur, *ibid* **36** , 491 (1967).
 - [12] V.A. Antonov, Vest. leningr. gos. Univ. **7** , 135 (1962).
 - [13] D. Lynden-Bell and R.Wood, 1968, MNRAS, **138**, 495. D. Lynden-Bell. Mon. Not. R. Astron. Soc. **136** 101 (1967).
 - [14] D. Lynden-Bell and R. Wood, Mon. Not. R. Ast. Soc. **138** , 495 (1968).
 - [15] W. Thirring, Z. Phys. **235** , 339 (1970).
 - [16] L. Velazquez and F. Guzman, e-print (2001) [cond-mat/0107214].
 - [17] L. Velazquez and F. Guzman, e-print (2001) [cond-mat/0107439].
 - [18] L. Velazquez and F. Guzman, Phys. Rev. E **65** (2002) 046134; e-print (2001) [cond-mat/0107441].
 - [19] L. Velazquez, R. Sospedra, J.C. Castro and F. Guzman, e-print (2003) [cond-mat/0303456].
 - [20] J. Binney and s. Tremaine, *Galactic Dynamics* (Princeton Series in Astrophysics, Pricenton, NJ, 1987).
 - [21] P. H. Chavanis, C. Rosier and C. Sire, preprint (2001) [cond-mat/0107345].